Scanning Microscopy

Volume 9 | Number 1 Article 11

1-21-1995

Scanning Electron Microscopy and Transmission Electron Microscopy Aspects of Synergistic Antitumor Activity of Vitamin C - Vitamin K3 Combinations Against Human Prostatic Carcinoma Cells

Jacques Gilloteaux
Northeastern Ohio Universities College of Medicine

James M. Jamison
Northeastern Ohio Universities College of Medicine

Meenaxi Venugopal
Northeastern Ohio Universities College of Medicine

David Giammar
Northeastern Ohio Universities College of Medicine

Jack L. Summers
Northeastern Ohio Universities College of Medicine

Scanning Microscopy, Vol. 9, No. 1, 1995 (Pages 159-173) 0891-7035/95$5.00+.25
Scanning Microscopy International, Chicago (AMF O'Hare), IL 60666 USA

SCANNING ELECTRON MICROSCOPY AND TRANSMISSION ELECTRON MICROSCOPY ASPECTS OF SYNERGISTIC ANTITUMOR ACTIVITY OF VITAMIN C - VITAMIN K_3 COMBINATIONS AGAINST HUMAN PROSTATIC CARCINOMA CELLS

Jacques Gilloteaux[1,*], James M. Jamison[2], Meenaxi Venugopal[1], David Giammar[2] and Jack L. Summers[3]

Departments of Anatomy[1], Microbiology and Immunology[2], and Urology[3],
Northeastern Ohio Universities College of Medicine, Rootstown, Ohio 44272, U.S.A.

(Received for publication June 26, 1994 and in revised form January 21, 1995)

Abstract

A MTT/formazan assay was used to evaluate the antitumor activity of vitamin C (Vit C), vitamin K_3 (Vit K_3), or vitamin C:vitamin K_3 combinations against a human prostatic carcinoma cell line (DU145). Both Vit C and Vit K_3 alone exhibited antitumor activity, but only at elevated doses. When Vit C and Vit K_3 were combined at a C:K_3 ratio of 100:1 and administered to the carcinoma cells, the 50% cytotoxic concentrations (CD_{50}) of the vitamins decreased 10- to 60-fold. Subsequently, the DU145 cells were examined with transmission and scanning electron microscopy (TEM and SEM) following a 1 hour treatment with Vit C, Vit K_3, or Vit C/K_3 combined at their 50% cytotoxic dose. Our morphological data suggest that vitamin treatment with individual vitamins affects the cytoskeleton, the mitochondria, and other membranous components of the cell. Treatment with the vitamin combination appears to potentiate the effects of the individual vitamin treatment. Specifically, there are abundant necrotic cells. The surviving cells display morphological defects characteristic of cell injury.

Key Words: Prostate carcinoma, vitamin C, vitamin K_3, cytotoxicity, ultrastructure, ruthenium tetroxide.

*Address for correspondence:
Jacques Gilloteaux
Department of Anatomy,
NEOU College of Medicine,
P.O. Box 95,
Rootstown, OH 44272, U.S.A.
Telephone number: 216 325 2511
FAX number: 216 325 7943

Introduction

Prostatic adenocarcinoma is the most frequently diagnosed cancer in males and the second leading cause of cancer related mortality in the United States (Moon, 1992). While a variety of treatment modalities, chemotherapy, radiation and biological response modifier therapy have been employed in an effort to manage prostatic adenocarcinoma, none of these regimens has proven to be efficacious. These observations point to the need for the development of an effective regimen for treating hormone-independent prostate cancer. Due to their low systemic toxicity, vitamins and combinations of vitamins have been evaluated for their antineoplastic activity.

Taper and coworkers (Noto *et al.*, 1989) found that co-administration of a Vitamin C (Vit C) and Vitamin K_3 (Vit K_3) combination (in a Vit C:Vit K_3 ratio of 100:1) to a variety of carcinoma cell lines resulted in equivalent antineoplastic activity at concentrations that were 10-50 times lower than when either vitamin was administered alone. The potentiation and specificity of the antitumor activity were ascribed to the possible generation of peroxides followed by membrane lipid alteration, DNase activation and DNA destruction by the Vit C and K_3 combination in the catalase-deficient cancer cells.

The purpose of this report is to evaluate Vit C, Vit K_3, and the Vit C:Vit K_3 combination for their antitumor activity against a human prostatic cell line (DU145) and to document morphological changes to subcellular compartments following a one hour vitamin treatment. Delayed cytotoxic and morphological effects of vitamins against DU145 cells have been evaluated and will be submitted elsewhere in the near future (Venugopal *et al*, in preparation).

Materials and Methods

Cell culture procedure

Human prostatic carcinoma cells (DU145 cell line) were purchased from the American Type Culture Collection (ATCC, Rockville, MD). After reception of the

Table 1. Antitumor activity of vitamins with coincubation with DU145 cells.

Coincubation Period	Vitamins alone		Vitamins Combinations		Enhancement of antitumor activity (n-fold)
	Vit C 50% cytotoxic dose (μM)	Vit K_3 50% cytotoxic dose (μM)	Vit C 50% cytotoxic dose (μM)	Vit K_3 cytotoxic dose (μM)	
5 day	2455 ± 28	12.9 ± 0.8	122 ± 15.6	1.22 ± 0.16	20
1 hour	6009 ± 8	77.2 ± 2.9	312 ± 4.0	3.12 ± 0.006	25

FIC = $CD^A_{50}{}^{comb}/ CD^A_{50}{}^{alone} + CD^B_{50}{}^{comb}/ CD^B_{50}{}^{alone}$, where FIC is the fractional inhibitory concentration, $CD^A_{50}{}^{alone}$ and $CD^B_{50}{}^{alone}$ are concentrations of each drug alone producing CD_{50}; $CD^A_{50}{}^{comb}$ is the concentration of drug A in combination with drug B yielding CD_{50}, and $CD^B_{50}{}^{comb}$ is the concentration of drug B in combination with drug A yielding CD_{50}. $FIC_{1\ hour} = 0.093$ and $FIC_{5\ day} = 0.145$.

frozen cells, they were thawed and centrifuged at 1000 rpm for 10 minutes. Following removal of the supernatant, DU145 cells were resuspended in 90% Minimum Essential Medium (MEM; Eagle, Gibco Labs., Grand Island, NY) supplemented with 10% fetal bovine serum (FBS; GIBCO), 50 μg/ml gentamicin sulfate (Sigma Chem. Co., St. Louis, MO) and grown in flasks until confluent.

Microtiter tetrazolium (MTT) assay

Corning 96-well titer plates were seeded with tumor cells (5.0 x 10^3/well) suspended in 100 μl MEM containing 10% FBS. The cells were then incubated at 37°C in 5% CO_2 for 24 hours. Tests solutions (8000 μM Vit C, 500 μM Vit K_3, and 80 μM Vit K_3/8 mM Vit C) were serially diluted with phosphate buffered saline (PBS) in 12 two-fold dilutions. Each dilution was added to 7 wells of the titer plates and incubated at 37°C in 5% CO_2 for 5 days. Following vitamin treatment and incubation period, host cell toxicity was assessed using the MTT assay in a microtiter plate reader (Alley *et al.*, 1988): 50 μl of 10 mM tetrazolium salt (3-[4,5-dimethylthiazol-2-yl]-2,5-diphenyltetrazolium bromide) was added to each well. The microtiter plates were then incubated at 37°C in 5% CO_2 for 4 hours. Following incubation, all but 20 μl of the supernatant was removed from the wells and replaced by 150 μl of dimethyl sulfoxide (DMSO; Sigma). Once the cells were solubilized, the absorbance of each well was read with a Bio Kinetics Reader (Model EL340; Bio-Tek Instruments, Winooski, VT) at 540 nm and 630 nm to eliminate background. The last six wells of the first column were used as MEM/tetrazolium blanks. All the wells in the last column of each microtiter plate lacked cells and were used for the drug blanks. Sham-treated cells were used as the negative controls. Following linear regression, the line of best fit was determined and the 50% cytopathic dose (CD_{50}) was calculated (Table 1). The fractional inhibitory concentration index (FIC; Sühnel, 1990) was employed to evaluate synergism, additivism, and antagonism. Using the same concentration of Vit C, Vit K_3 and the combination of the two vitamins, a similar MTT assay was evaluated after a 1 hour treatment (Table 1).

Treatments and preparation for microscopy

Two 12-mm circular glass coverslips or two 100-mesh gold grids were placed in a 35 mm Petri dish.

Control DU145 cells (Figures 1-6).

Figure 1. Scanning electron micrograph of sham-treated cells reveal the typical spherical shape of the cells. Bar = 10 μm.

Figure 2. Scanning electron micrograph of sham-treated cells illustrating a flat cell. Open arrow: contacting filopodia. Bar = 5 μm.

Figure 3. Transmission electron micrograph of a sham-treated cell. Note the lobed nucleus and large glycogen deposits (*), lysosomes/residual bodies near the nucleus and the abundant mitochondria. Note a adjacent cell with a characteristic intracellular lumen (i). Bar = 5 μm.

Figure 4. Transmission electron micrograph of the cytoplasm where TRS (arrows) are depicted among other organelles. Arrowhead: mitochondria. Bar = 1 μm.

Figure 5. Enlarged nucleus of DU145 cell showing 2 nucleolar bodies, each containing 2-4 fibrillar centers (curved arrow). Bar = 1 μm.

Figure 6. Transmission electron micrograph of enlarged perikaryal annulate lamellae. a: annulate lamellae; n: nucleus; arrowhead: mitochondria. Bar = 200 nm.

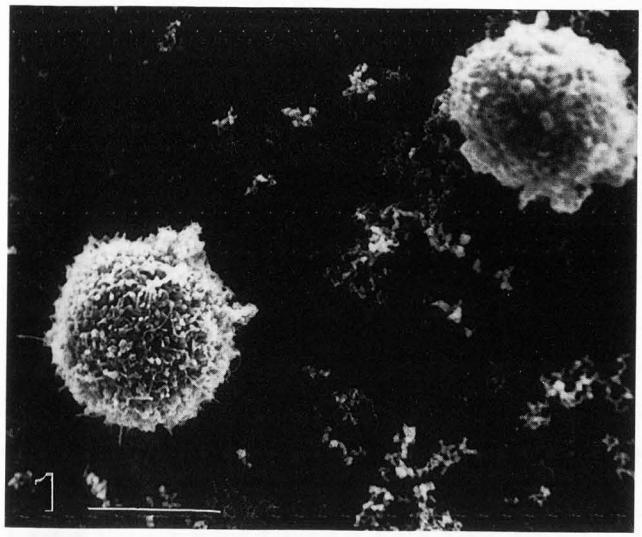
1

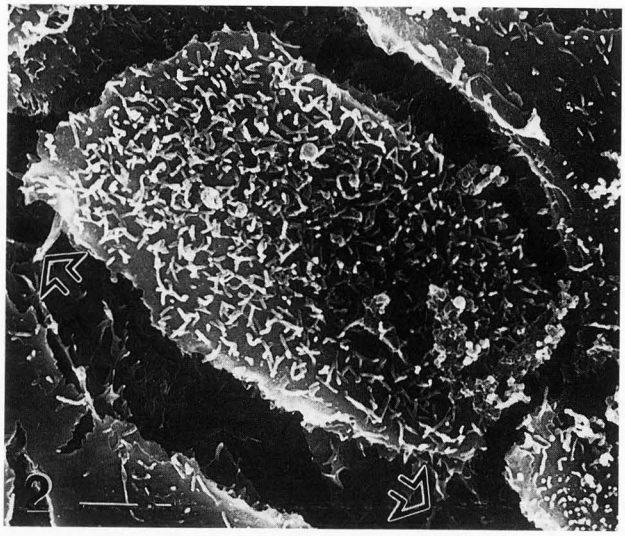
2

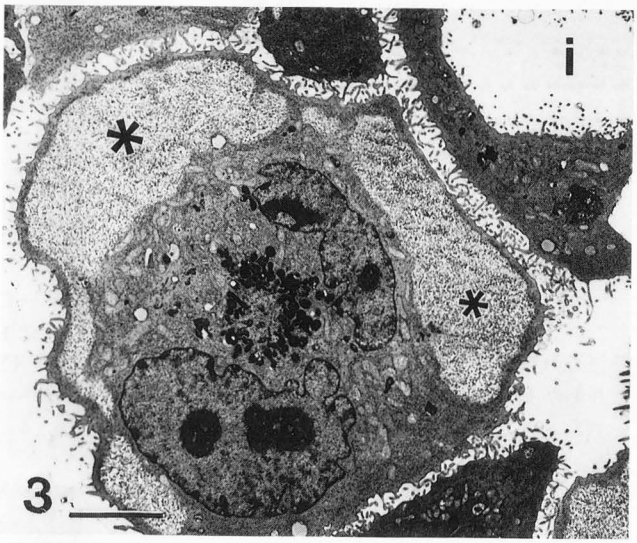
i
3

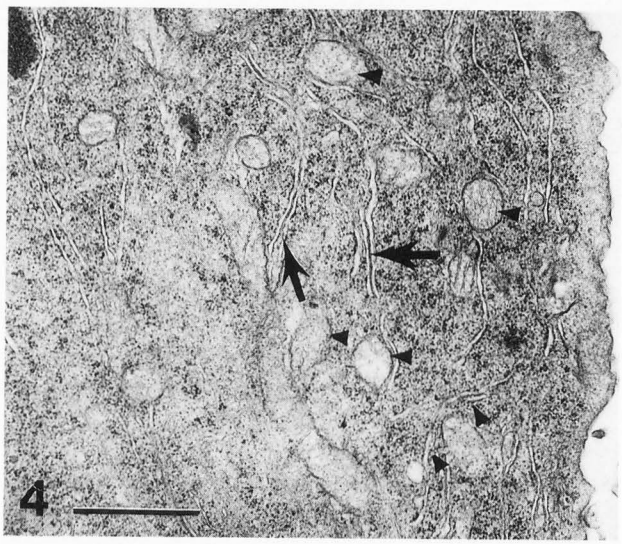
4

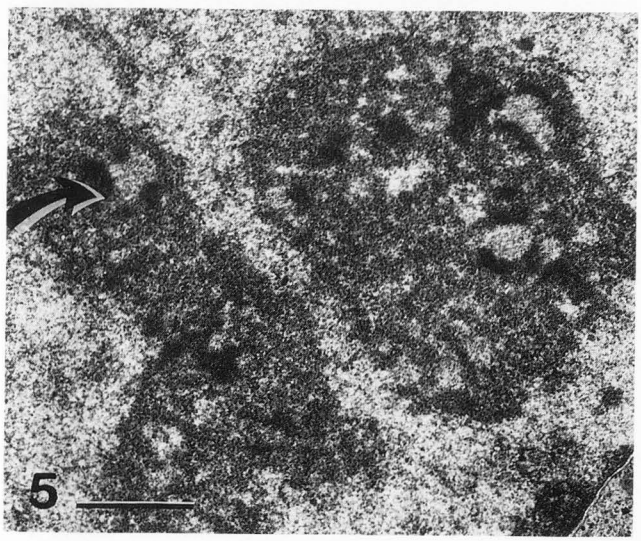
5

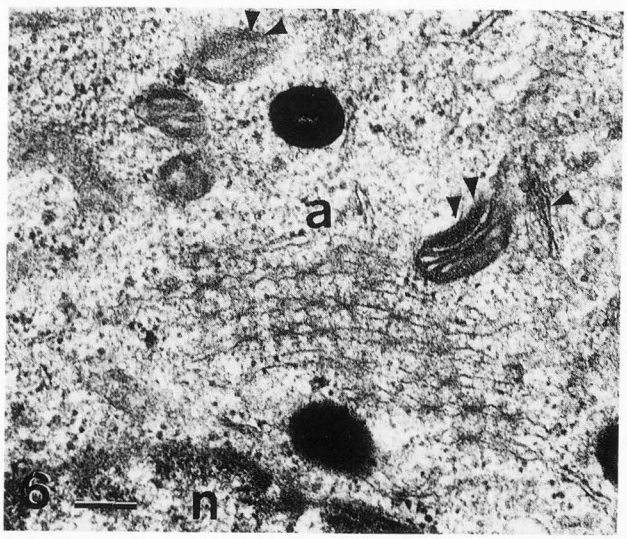
a
6
n

Each Petri dish was seeded with 1.0 x 10^6 DU145 cells suspended in MEM containing 10% FBS. After 24 hour incubation at 37°C in 5% CO_2, MEM was removed and the cells were washed once with 3 ml of PBS (pH 7.2). The cells were then overlaid with 2 ml of MEM containing either Vit C (6007 μM), Vit K_3 (77.2 μM), or Vit C:Vit K_3 (312 μM : 3.1 μM) combination. These values corresponded to the CD_{50} doses determined by MTT analysis. MEM-treated DU145 cells were used as the negative control. After 1 hour of incubation at 37°C and 5% CO_2, the vitamins were removed from the cells and the cells were rapidly washed twice with 3 ml of PBS. Glass coverslips and grids covered by DU145 cells were transferred to another Petri dish for scanning electron microscopy (SEM). The DU145 cells that adhered to the Petri dish following vitamin treatment were harvested by soaking them free from the monolayer with no-zyme (JRH Bioscience, Lenexa, KS), centrifuged at 1000 rpm for 10 minutes and then prepared for transmission electron microscopy (TEM).

Scanning electron microscopy (SEM) preparations

DU145 cells on the glass coverslips and grids were covered with 3.2% buffered glutaraldehyde solution (0.1 M Na cacodylate; pH 7.32) for 10 min at 4°C (Allen, 1983; Glauert, 1984; Prince *et al.*, 1993). After two rapid washes with sucrose-cacodylate buffered solution (SC), the preparations were postfixed for 30 minutes at room temperature in 1% aqueous solution of osmium tetroxide-ruthenium tetroxide (1:1). The rationale in using ruthenium tetroxide (RuO_4) with osmium tetroxide (OsO_4) is to allow the fixation to penetrate rapidly into cell structures and to compound its fine fixative quality with that of osmium tetroxide (Gaylarde and Sarkany, 1968; Gilloteaux and Naud, 1979; Hayat, 1970). Following fixation, the samples were then washed four times with the SC solution and dehydrated through a graded series of ethanol. Critical-point drying was performed in a Polaron E 3000 apparatus (Polaron/Biorad, Cambridge, MA) using liquid CO_2 as transitional fluid. After gluing each cover slip on an aluminum holder with conductive silver paint (high purity silver paint; SPI, West Chester, PA) or each gold grid with double-side adhesive tape (Avery Dennison, Azusa, CA) and paint; all the SEM samples were sputter-coated with a Hummer VI-A (Anatech Ltd., Alexandria, VA) with a 20 nm-thick gold layer before observation with a JEOL JSM-35C SEM operated at an accelerating voltage of 15 kV.

Transmission electron microscopy (TEM) preparations

The supernatant was removed and replaced by the same buffered glutaraldehyde solution as that used for the SEM preparations except that the fixation was carried out at room temperature for 1 hour. After two rapid rinses in SC solution, postfixation was done for 1 hour at room temperature with 1% aqueous osmium tetroxide solution. The pelleted cells were washed in the SC solution before dehydration in graded ethanol, and processed in PolyBed epoxy resin (Polysciences, Warrington, PA). One-micrometer thick sections were stained by toluidine blue and selected areas were collected as ultrathin sections on 75-and 100-mesh hexagonal copper grids (SPI). The sections were contrasted by uranyl acetate and lead citrate and were examined in a JEOL 100S transmission electron microscope operated at an accelerating voltage of 80 kV.

Vitamin C treated DU145 cells (Figures 7-13).

Figures 7 and 8. Scanning electron micrographs of DU145 cells with extended lamellipodia (**Fig. 7**), reticulated (r) filopodial field and extensive blebbing (**Fig. 8**). Bars = 10 μm.

Figure 9. This transmission electron micrograph shows cytoplasmic vacuolization and residual bodies randomly scattered throughout the cytoplasm of several cells. *: glycogen deposits. Bar = 5 μm.

Figure 10. Enlargement of peripheral cytoplasmic region demonstrating reticulated microvillar-like anastomoses, membranous blebs (b) perikaryal residual bodies (arrow) and mitochondria (arrowhead). Open arrow: onion-like body. Bar = 1 μm.

Figure 11. Enlargement of the cytoplasmic glycogen deposits (*) loosely surrounded by a membranous (lysosomal-like) structure (arrows). Extracted fatty deposits (f) are also present. Bar = 1 μm.

Figure 12. An example of condensed nucleolus showing nucleolar chromatin condensation (curved arrow). Bar = 1 μm.

Figure 13. Transmission electron micrograph of perinuclear cytoplasm with anastomosed and fragmented TRS (open arrow) and condensed nuclear envelope. Bar = 200 nm.

Results

A MTT-microtiter tetrazolium assay has been employed to determine if Vit C and Vit K_3 exhibit synergistic antitumor activity against prostatic carcinoma. When the test agents are incubated with DU145 cells for 1 hour, the CD_{50} of Vit C alone is 6009 μM and the

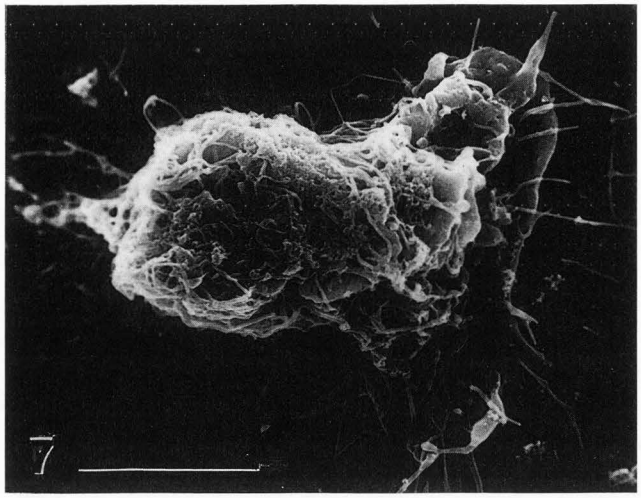
7

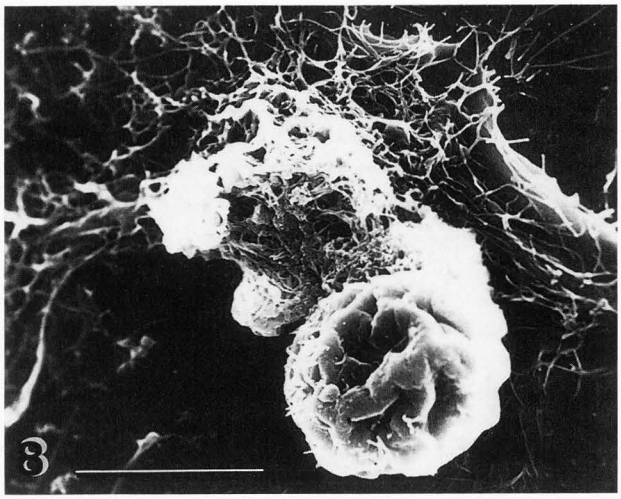
8

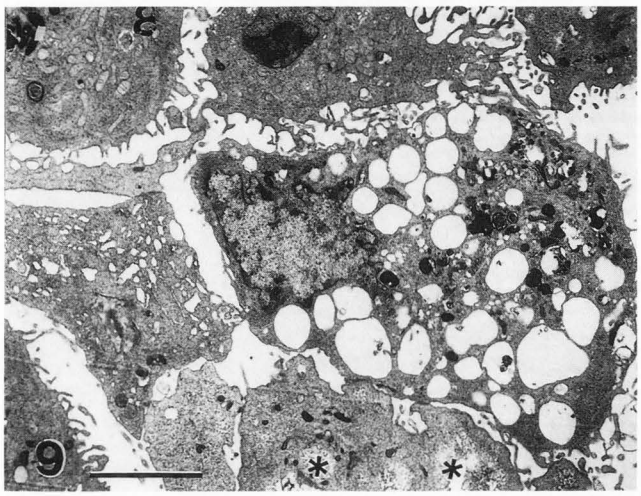
9

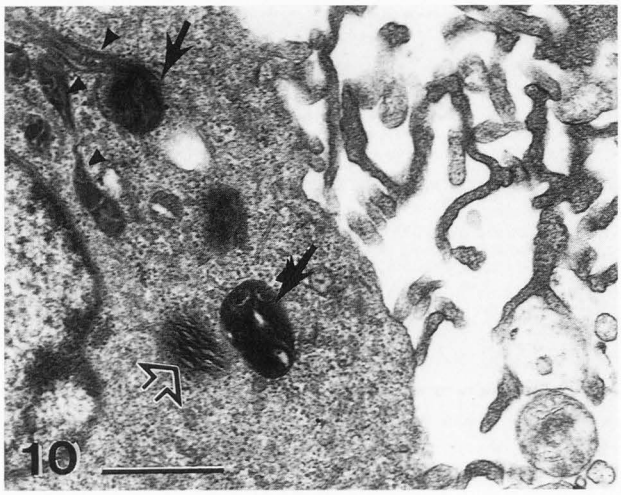
10

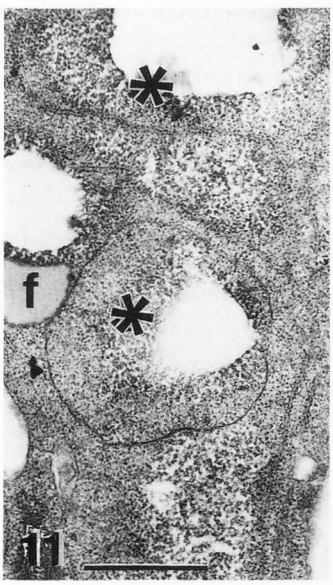
f
11

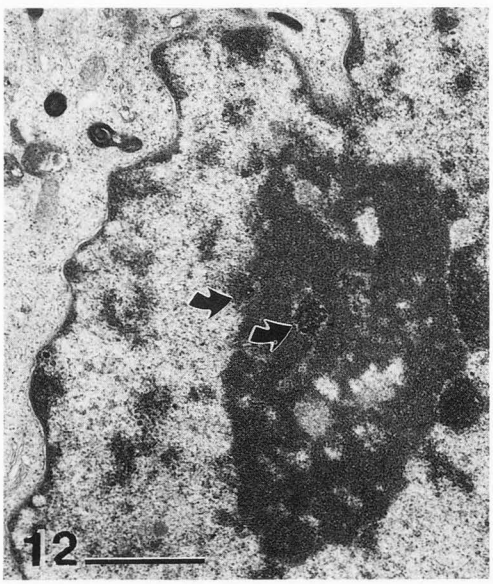
12


13

CD_{50} of Vit K_3 alone is 77.2 μM. When Vit C is combined with Vit K_3 to produce a Vit C/Vit K_3 ratio of 100:1, the ratio of CD_{50} for the two vitamins is 312: 3.12. These results demonstrate that when Vit C is combined with Vit K_3, the CD_{50} of Vit C decreases from 6009 μM to 312 μM (a 20-fold decrease), while the CD_{50} of Vit K_3 decreases from 77.2 μM to 3.12 μM (a 25-fold decrease). The FIC index (Sühnel, 1990) has been employed to evaluate synergism, additivism or antagonism. A FIC < 1.0 indicates the combination is synergistic, while a FIC > 1.0 indicates the combination is antagonistic. A FIC ≈ 1.0 indicates the combination is additive or indifferent. Employing these criteria, Vit C and Vit K_3 exhibit a marked synergism (FIC $= 0.093$) when they are administered at an Vit C/Vit K_3 ratio of 100:1.

For ease of comparison, scanning and transmission electron micrographs are presented together: control DU145 cells (Figs. 1-6), Vit C-treated DU 145 cells (Figs. 7-13), Vit K_3-treated DU145 cells (Figs. 14-20) and Vit C/Vit K_3-treated cells (Figs. 21-29).

Scanning electron microscopy

Untreated (control) DU145 cells (Figs. 1 and 2): Untreated DU145 cells are typically spherical and have diameters ranging from 12 to 17 μm (Fig. 1). These cells show a narrow rim of lamellar cytoplasm from which discrete surface specializations in the form of radial lamellipodia and/or filopodia originate. While the former can barely be detected at low magnifications of SEM, the latter can be seen to originate from one sector of the cell. The lamellipodia can protrude up to 2 μm outside the main cell surface, while the filopodia can measure up to 15 μm in length and 0.2 μm in diameter. Control cells show a tendency to overlap and aggregate in groups of up to 13. These cells, or colonies, appear to be flat when they are confluent and can attain a diameter of 30 μm in their long dimension and 20 to 30 μm in their shorter dimension (Fig. 2). Due to the flattened appearance of confluent cells, it is difficult to appreciate their width. Under such conditions, round cells can sometimes be detected overlapping the flat cells. During cell aggregation, adjacent cells display complementary interlocking three dimensional structures (same size and length) and have focal contact with very short filopodia (Fig. 2).

Vitamin C-treated DU145 cells (Figs. 7 and 8): Vit C-treated DU145 cells are pleomorphic. Vit C-treated cells also have a tendency to form colonies like the untreated DU145 cells. Contacts between adjacent cells are similar to control cells. However, profound morphological alterations can be detected in the form of membrane extensions or radial appendages, i.e., lamellipodia- and filopodia-like extensions as well as irregular and unequal projections from the cell surface. When lamellipodia are present, they can reach up to 4 to 5 μm in length. In some parts of the cell surface, lamellipodia can be observed as ruffles with filopodia arising randomly from the upper ridges of the lamellipodia (Figs. 7 and 8). The filopodia are typically tenuous and can show a reticulated aspect (Fig. 8) which is confirmed by TEM (Fig. 10). These filopodia can be as large as 10 μm in length and 0.2 μm in diameter. Vit C-treated cells display cell shapes varying from almost spherical to almost flattened and, in some cases, even crenate in appearance. Frequently, the nuclear region protrudes outward from the cell surface. These cells are sometimes doughnut shaped (similar to Vit K_3-treated cells shown in Fig. 22).

Vitamin K_3-treated DU145 cells (Figs. 14, 15 and 18): Vit K_3-treated cells show a large lamellar cytoplasm when they are confluent. When ovoid, these cells, like the Vit C-treated cells, show a tendency to aggregate. These cells can also be oblong in appearance and possess surface modifications like lamellipodia, pseudopodia, filopodia and blebs of irregular size and

Vitamin K_3- treated DU145 cells (Figures 14-20).

Figures 14 and 15. Vitamin K_3-treated cells with predominant membranous blebs and thick curly pseudopodia which depicts zeiosis. This suggests K_3-induced alterations in the cytoskeleton of the cell. Bars = 25 μm (Fig. 14) and 10 μm (Fig. 15).

Figure 16. Closer examination of a residual body indicates that it has a whorled appearance and originates from damaged mitochondria (arrow). Bar = 1 μm.

Figures 17 and 19. Intense cytoplasmic vacuolization and residual bodies are randomly scattered throughout the cytoplasm. In contrast to Vit C treatment, the glycogen deposits (*) appear unaffected by the vitamin treatment. The cells display long cytoplasmic digitations. Notice the enlarged nucleolus. Bars = 10 μm.

Figure 18. Scanning electron micrograph of a DU145 Vit K_3-treated cell showing many irregular blisters and entangled filopodia. Dilated membranous blebs surround the main cell body thereby giving it a petal-like appearance. Bar = 10 μm.

Figure 20. Enlarged view of a dense body originating from a mitochondrium (arrow). Apparent curved cisternae can be observed adjacent to the dense body. The morphology of these cisternae resembles TRS. Bar = 200 nm.

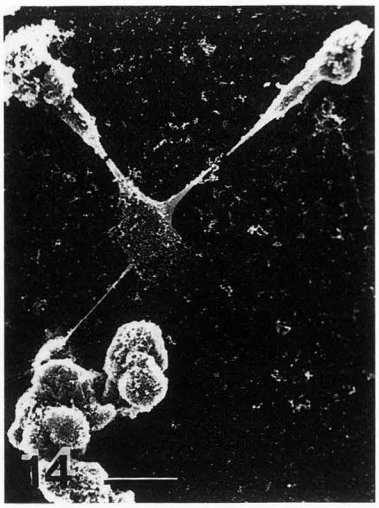
4

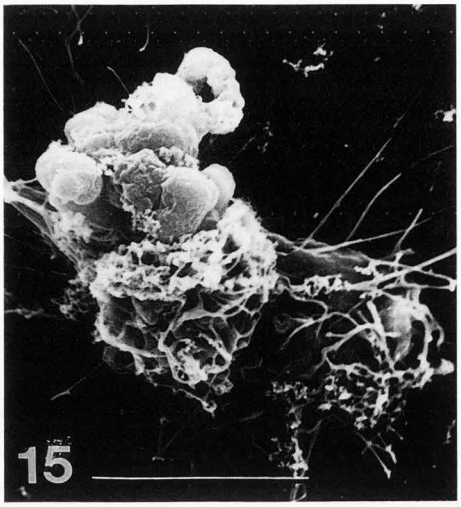
15

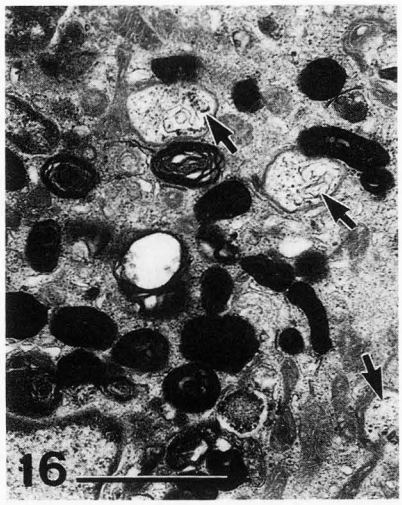
16

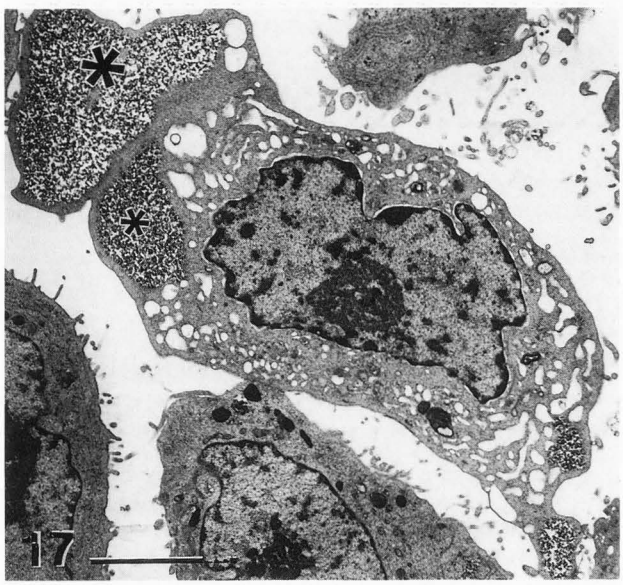
17

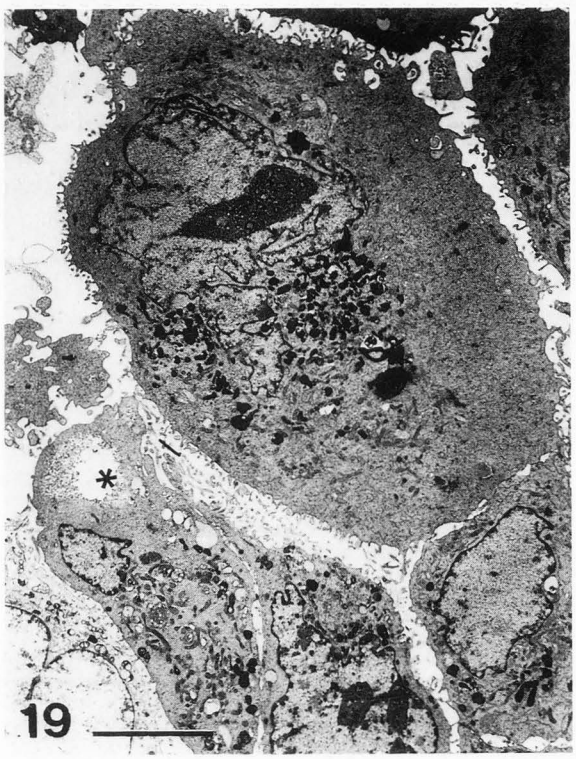
19

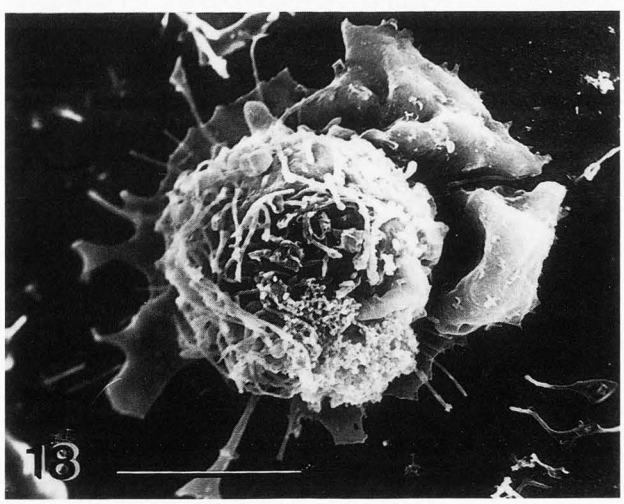
18

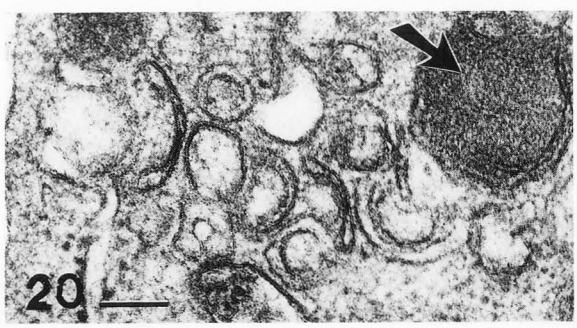
20

Some of these extensions are similar to those observed in Vit C (compare Fig. 15 with Figs. 7 and 8). In addition, many cells show numerous large blebs budding from the same region of the cell as surface modifications and results in further disorganization of the outline of the cells. Blebs can measure up to 3 μm in diameter. In addition, long or wavy pseudopodia can also be detected (Figs. 14 and 15). Filopodia are more than 10 μm in length and typically 0.2-0.3 μm in diameter. Isolated cells exhibit irregular pseudopodial and filopodial processes and attempt to contact other cells via such processes (Fig. 14). When cells do not make contacts with neighboring cells, they form wide and radial lamellar cytoplasmic arms of about 5 μm in width giving the cell a rosette appearance. Alternatively, these cell extensions could be indicative of zeiosis (Fig. 18). It is not unusual to also observe many doughnut-shaped cells and necrotic cells in a field of view.

Vitamin C/Vitamin K_3-treated DU145 cells (Figs. 21, 22 and 29): These cells appear round to ovoid. Vit C/Vit K_3-treated cells are attached to the substrate by means of a basal array of narrow and radiating lamellar cytoplasmic arms arising from the basal portion of each cell. Long filopodia can be seen to arise from these arms (Figs. 21 and 22). These cells form large clusters. Surface modifications like blisters, irregular lamellipodia, and filopodia cover the entire surface of these cells. Necrotic cells can also be observed in a field of view. Such necrotic cells exhibit either cell remnants from which nuclei have been extruded (Fig. 22) or a severed nuclear region which can still be detected among cytoplasmic fragments (Fig. 29).

Transmission electron microscopy

Control DU145 cells (Figs. 3-6): At low magnifications, DU145 cells display a round to polygonal profile and are coated with short (0.5 μm), microvilli-like digitations of equal height. Cells which exhibit polygonal profiles contact each other by intermingling their microvillar extensions. In some instances, one can detect small to large intracellular lumens delineated by microvillar-like surfaces (Fig. 3).

The nucleus is generally multi-lobed and often shows deep cytoplasmic indentations. Many nucleoli contain multiple fibrillar centers, i.e., nucleolar organizers regions (NORs). This excess in the number of NORs is characteristic of tumor cells (Fig. 5; Schwarzacher and Wachtler, 1993). Abundant electron dense residual bodies are present in the perinuclear regions. These residual bodies are located in either the major concavity of the perikaryons or in a concentric, non-peripheral distribution (Figs. 3 and 6).

Mitochondria occupy a large volume of each cell, show a pale matrix and are dilated with diameters as large as 0.5 μm (Figs. 3, 4 and 6). Large cytoplasmic deposits of glycogen can be detected in many DU145 cells. They are often ectoplasmic and can occupy as much as half of the cell profile (Fig. 3).

RER and associated polysomes are easily detectable and dispersed throughout the cell cytosol. These cells contain abundant SER, some of which resembles tubuloreticular structures (TRS). These TRS are often detected as elongated (1 to 3.5 μm long) meandering or sinuous structures in the peripheral cytoplasm (Fig. 4). A small number of minute pale to electron-lucent spaces, which are lipid-containing vacuoles (Fig. 3), are also present. These fatty deposits are also observed in treated cells (Figs. 11 and 24). Close examination of the DU145 control cells allowed us to often observe annulate lamellae in their perikaryons (Fig. 6). These cellular substructures are often detected in tumor cells (Ghadially, 1988).

Vitamin C-treated DU145 cells (Figs. 9, 10, 11, 12 and 13): As a result of Vit C treatment, the cells lose their spherical shape and acquire a more elongated profile with irregularly-shaped, branching extensions and intricate unequal surface folds. Arising from these extensions, one can note more delicate microvillar-like structures (Fig. 9) and membranous blebs containing foam-like structures which are outlined by a membranous boundary (Fig. 10). These extensions appear in an anastomosing and reticulated pattern (Fig. 10).

Vitamin C/K_3- treated cells (Figures 21-29).

Figure 21. Illustration of elongated cells with many surface blisters and blebs. Lamellipodia (curved arrow) display clusters of excrescences. Bar = 10 μm.

Figure 22. An example of a doughnut shaped cell with numerous surface extensions and bulging cytoplasm (b). Bar = 10 μm.

Figures 23 and 24. Illustration of Vit C/K_3-treated demonstrating aggregates of swollen mitochondria with defective matrix (small arrow). f: fat; arrowhead: RER; large arrows: residual body. Bars = 1 μm.

Figure 25. Transmission electron micrograph of nucleolus with many fibrillar centers. Curved arrow: nucleolar-associated chromatin. Bar = 1 μm.

Figure 26. Illustration of a vacuolated cell with condensed nucleolus. Notice an example of glycogenic deposit surrounding an extracted fatty deposit (*). Cytoplasmic extrusions typical of zeiosis (arrow) can also be seen. Bar = 10 μm.

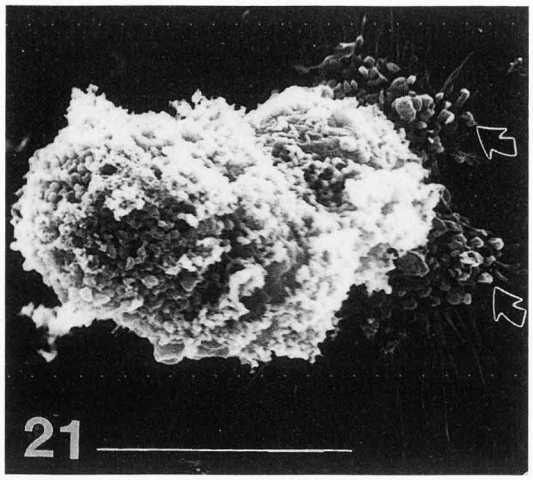
21

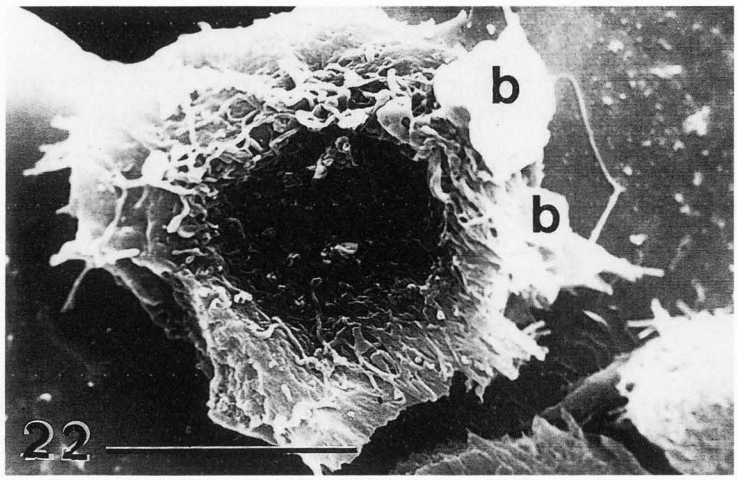
b
b
22

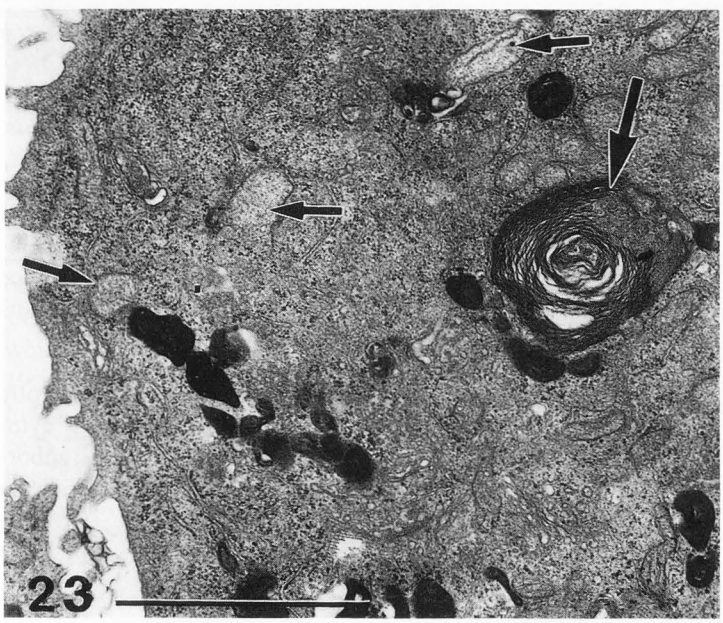
23

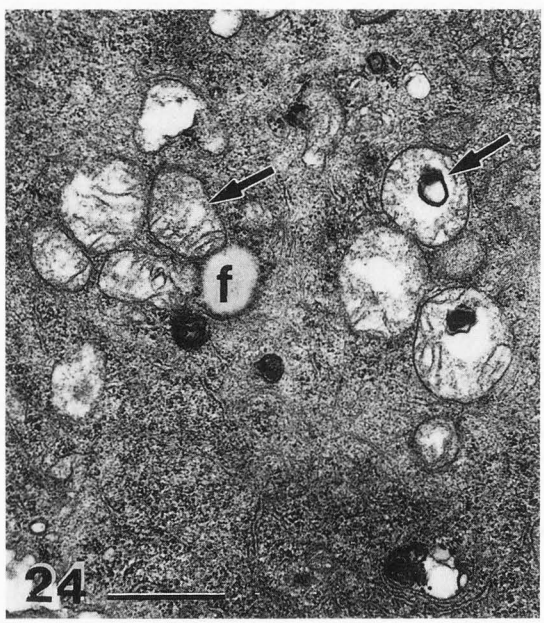
f
24

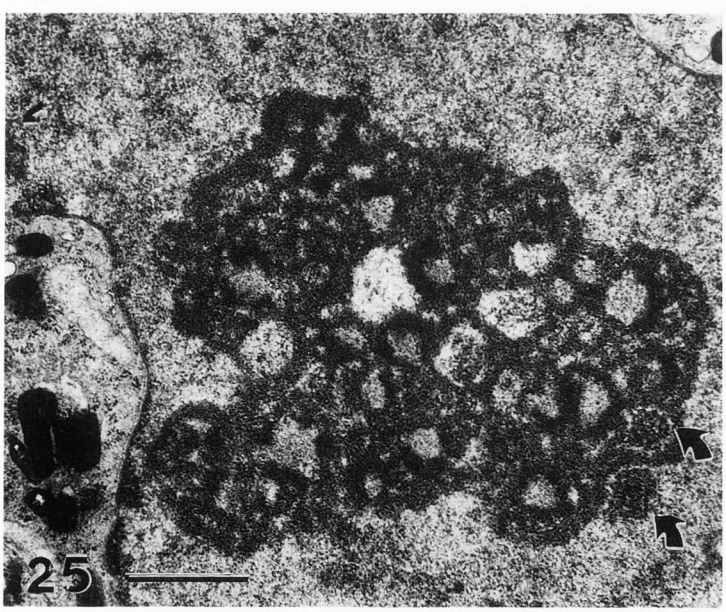
25

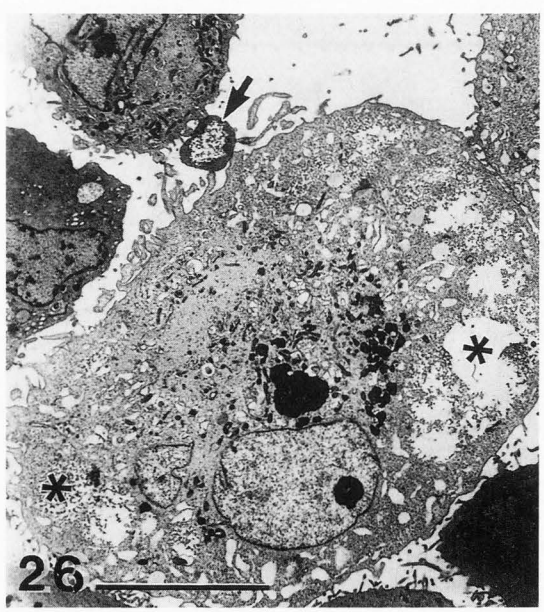
*
*
26

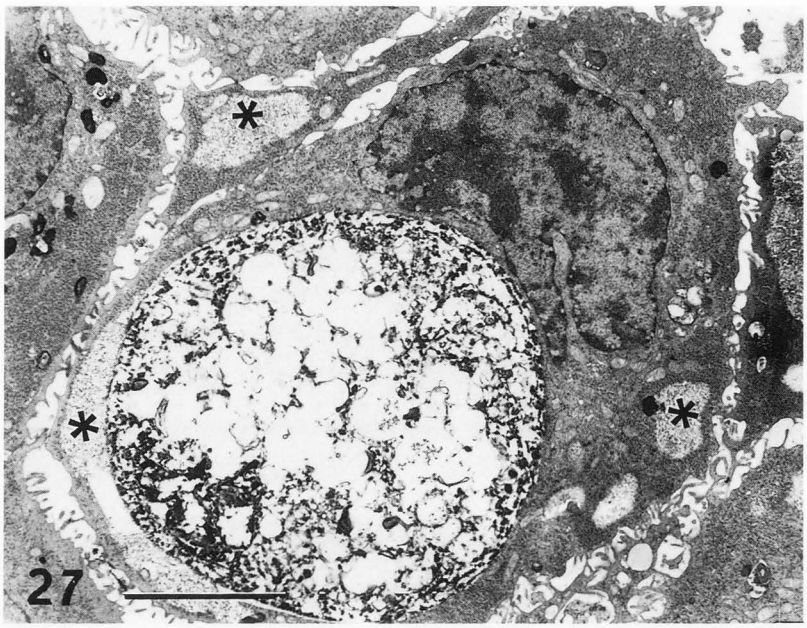

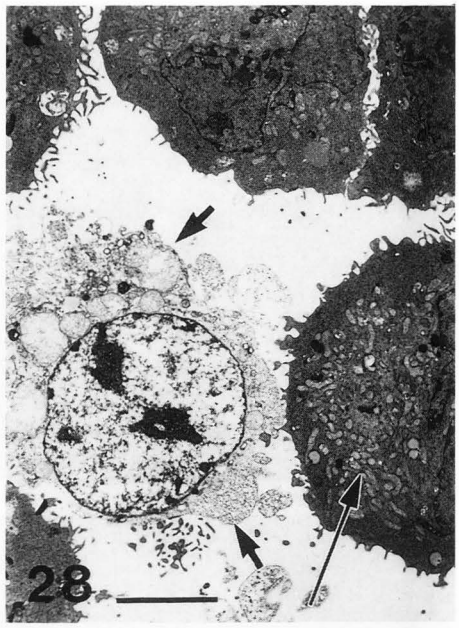

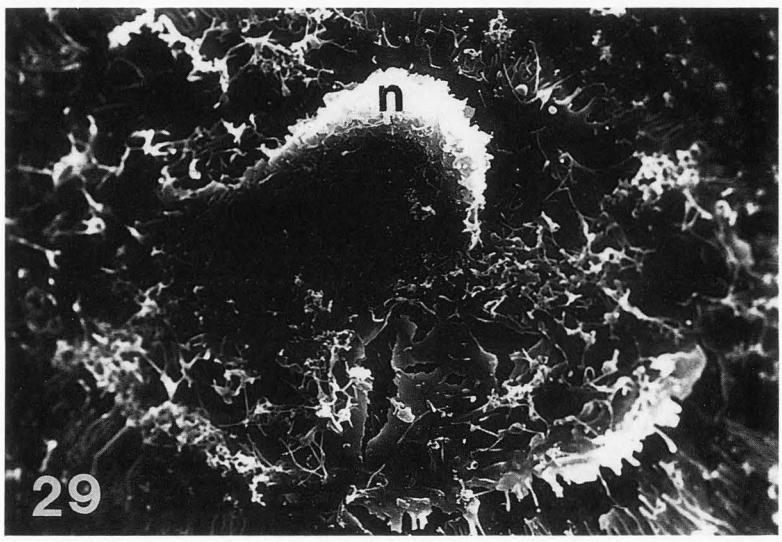

Figure 27. An example of a cell containing an extremely large lysosomal vacuole containing heterogenous membranes and clumped material. Notice the intact peripheral glycogen deposits (*). Bar = 5 μm.

Figure 28. Illustration of a necrotic cell in the process of expelling cytoplasmic buddings. Notice the neighboring cell whose cytoplasm is rich in swollen mitochondria (long arrow as shown in Figure 24). Arrows: budding excrescences. Bar = 10 μm.

Figure 29. Scanning electron micrograph of a necrotic cell with segregated nuclear bulging (n) which is surrounded by cytoplasmic debris. Bar = 10 μm.

Vit C-treated cells show nuclei with more rounded profiles than control DU145 cells. Vacuolated and swollen cells possess eccentric nuclei and display characteristics of cell injury indicating an early step of cell degeneration (Fig. 9). The nuclear indentations appear to be fewer and are less deep than in control cells. A striking feature is the nucleolus which is enlarged, often single, and has a moth-eaten aspect among finely dispersed heterochromatin. Fine fibrillar centers can be detected among more electron dense material which probably consists of the dense fibrillar component. There is an apparent condensation of perinucleolar chromatin within sections of the nucleolar bodies (Fig. 12). The overall electron density of the nucleolar components makes it difficult to distinguish the granular component. Although the granular component is present, it is dispersed among the aforementioned nucleolar substructures. The inner nuclear membrane shows a thick layer of heterochromatin (Fig. 13) when compared to the nuclei of control cells and Vit K_3-treated cells.

Following treatment, many cells display intense cytoplasmic vacuolization and residual bodies are randomly scattered among the cytoplasmic organelles as well as in the perikaryon (Figs. 9 and 10). Among the residual bodies, one observes condensed mitochondrial matrices and altered mitochondria which suggest a mitochondrial origin for these residual bodies. Other dense bodies appear in the form of onion-like bodies.

Cytoplasmic vacuolization appears within the glycogen patches and in the vicinity of lipid droplets (Fig. 11). Lipid droplets detected as empty spaces among the glycogenic stores are likely to be related to the procedures of fixation and dehydration (Glauert, 1984; Stein and Stein, 1971) and cytoplasmic vacuoles in the area of the glycogenic patches contain an electron lucent area (vacuole) that is circumscribed by a SER-like membranous structure which suggests a possible lysosomal genesis (Fig. 11). In addition, the perinuclear regions contain networks of anastomosing or fragmented TRS (Fig. 13). As in the control cells, the overall cytoplasm contains abundant fine electron dense granules which are probably ribosomes. Alternatively, many of these granules could represent ribosomes which have degranulated from the RER.

Vitamin K_3-treated DU145 cells (Figs. 16, 17, 19 and 20): Following Vit K_3 treatment, most cells appear ovoid or elongated and display smooth surfaces which are often free of microvillar-like surface profiles (Figs. 17 and 19). Most remaining cellular extensions are long and scattered along the cell surface. These morphological aspects confirm the SEM observations (Figs. 14, 15 and 18). An example of zeiosis (blebs containing, e.g., organelles and glycogenic stores) is depicted in Figure 17. Cells show membranous blebs and round ruffles which are several micrometers in diameter (Figs. 17 and 19 similar to what is observed in Figs. 26 and 27). At low magnification, cells appear to aggregate and large cells tend to surround the smaller ones within their extensions (Fig. 19). In addition, membranes exhibit numerous blebs which are delineated by a unit membrane. The large blebs or dilated ruffles do not appear to contain organelles, but do contain glycogen laden vacuoles which are surrounded by an electron dense cytoplasmic rim not thicker than 0.2 μm.

The nucleus is discretely lobed and the nucleoli of these Vit K_3-treated cells are significantly enlarged and can appear round or branching. Nucleolar bodies are enlarged when compared to those of untreated cells and range from 2 μm to 6 μm in diameter. There is an apparent condensation of the nucleolar chromatin within sections of the nucleolar bodies (Fig. 12). The heterochromatin is dispersed in small patches throughout the nucleoplasm and the nucleoli contain several fibrillar centers.

In addition to glycogen patches, the cytoplasm of Vit K_3-treated cells appears extensively vacuolated in the elongated cells and slightly vacuolated in the rounded cells. These rounded cells also possess a large number of dense bodies in their perikaryons (Figs. 17 and 19). At higher magnification, these electron dense structures appear to be vacuolated and non-vacuolated onion-like bodies. Upon closer examination of the same Vit K_3-treated DU145 cells, one can determine that most, if not all, of these dense bodies originate from mitochondrial alterations (Figs. 16 and 20). Enlarged and altered mitochondria can be detected among the dense bodies. These mitochondria have a pale matrix and disorganized cristae (Fig. 20). SER and dense bodies are seen in the cytoplasm. In addition, many small cisternae form a vacuolated network among these dense bodies. These cisternae are usually curved and measure about 45 to 300 nm in diameter or width and appear as sectioned TRS (Fig. 20). These cisternae are extensively developed in the elongated cells which surround the smaller cells.

Vitamin C/Vitamin K_3-treated DU145 cells (Figs. 23-28): Vit C/Vit K_3-treated cells appear round to ovoid and possess a high nuclear to cytoplasmic ratio. One reason for this type of change is that these cells appear to extrude large portions of their cytoplasm into protruding blebs. The outline of intact cells is clearly surrounded by numerous thin and thick irregular microvilli as well as by short ruffles or blebs of the cell surface (Figs. 23, 27 and 28). The cells that contact each other show more electron density and exhibit a more "intact" appearance than those which have not made such contact. These scattered cells appear to undergo necrosis associated with the aforementioned intense zeiotic blebbing of cytosolic fragments (Figs. 26 and 28). As was the case in SEM, it is quite common to find necrotic cells in TEM also (Figs. 26 and 28).

Nuclei of Vit C/Vit K_3-treated cells are lobed; they are larger and less condensed than the Vit C or Vit K_3-treated cells (Fig. 26). If the nucleoli are branched, then they occupy a large volume of the nucleoplasm (Figs. 25 and 28). Enlarged nucleoli show loose interstices with incomplete rings of dense fibrillar material. It is difficult to differentiate the nucleolar-associated chromatin from the nucleolar material proper (Fig. 25). The cytosol of Vit C/Vit K_3-treated cells is very granular with many of these granules corresponding to the size of ribosomes. The RER is scanty and only present in the form of minute membranous fragments adjacent to the damaged mitochondria (Figs. 23 and 24). As a result of degranulation of the RER, large quantities of ribosomes are dispersed between all the organelles of the cell (Fig. 24). The cytoplasm is moderately vacuolated and contains small (1-1.5 μm) to extremely large (4.0-6.5 μm) heterogenous vacuoles which can be in close contact with the nuclear envelope (Figs. 26 and 27). Lipid-containing vacuoles are not more than 1 μm in diameter and are electron lucent.

In some of the cells, the mitochondria display their orthodox substructure and are surrounded by networks of typical RER. However, most mitochondria are dilated, possess damaged cristae and contain a hetero-

geneous matrix (Figs. 24 and 28). Some of the apparently intact cells contain aggregates of typical mitochondria and dilated mitochondria (Fig. 24) which may occupy a large volume of the cytoplasm. All of these features may contribute to the vacuolated aspect of the cytoplasm.

However, as was the case in the Vit K_3-treated cells, all the cells observed in our preparation contained numerous dense residual bodies originating from the mitochondria. Some residual bodies can reach up to 3 μm in diameter. In addition, large (2 μm) lamellated onion-like bodies can be seen. Enormous heterogenous inclusions (up to 15 μm in diameter) can be found in some large cells. These inclusions represent large autophagosomes or heterophagosomes which can result from cannibalization of necrotic cells. Figure 26 demonstrates this type of event and also shows that large glycogenic reserve patches are still present in the cytoplasm following Vit C/Vit K_3 treatment.

Discussion

The DU145 cell line is a promising *in vitro* model for human prostatic carcinoma because it can be maintained in long term culture and its growth is hormone-independent (Chakraborty and Von Stein, 1986). DU145 cells in culture show rounded appearance especially when they are isolated and/or when ready for mitotic activity. It has been observed that DU145 and PC-3, both human prostatic adenocarcinoma cell lines, display characteristic bimorphism and appear phenotypically as rounded or flattened cells (Carruba *et al.*, 1989). Besides being a characteristic feature of germ cells, annulate lamellae are also found or induced in tumor cells (Ghadially 1988; Kessel, 1968, 1973, 1983) and are observed in untreated DU145 cells.

The results of *in vitro* studies demonstrate that Vit C exhibits a selective toxicity towards malignant melanoma cells (Bram *et al.*, 1980), human leukemia cells (Park *et al.*, 1980), neuroblastoma cells (Prasad *et al.*, 1979), and tumor ascites cells (Liotti *et al.*, 1984). The mechanism(s) responsible for the antitumor activity of Vit C are obscure, but may be related to the ability of Vit C to inhibit macromolecular synthesis to induce DNA strand breaks and cross-links (Noto *et al.*, 1989; Pavelic *et al.*, 1989).

Ultrastructural studies (Lupulescu, 1992) of Vit C-treated basal cell and squamous cell carcinoma cells revealed advanced cytolysis, cell disorganization, membrane disruption, mitochondrial alterations, and nuclear/nucleolar reduction as well as increased phagolysosome formation and collagen synthesis. Moreover, the TRS complexes (Ghadially, 1988; Orenstein, 1992), observed in the untreated cells, are often fragmented following this treatment. These results suggest that the antitumor activity of Vit C may be due to increased cytolytic and autophagic activity with vacuolated degeneration and the subsequent disruption of cellular membranes. Vit K_3 (menadione, 2-methyl-1,4-naphthoquinone) is a synthetic derivative of Vit K_1 that exhibits broad spectrum anticancer activity against human cancer cell lines and against human tumor explants which are refractory to other types of chemotherapy (Chlebowski *et al.*, 1985; Nutter *et al.*, 1991; Wu *et al.*, 1993). Administration of Vit K_3 is known to induce a variety of effects including: increased consumption of molecular oxygen and generation of superoxide, depletion of glutathione (GSH), oxidation of protein sulfhydryl groups in cytoskeletal proteins, alterations in pyridine nucleotide pools, decreases in mitochondrial and cellular ATP pools, effects on calcium homeostasis, and single-stranded DNA breaks (Gant *et al.*, 1988; Mirabelli *et al.*, 1989; Stubberfield and Cohen, 1989).

Ultrastructural studies (Bellomo *et al.*, 1990; Malorni *et al.*, 1991) of Vit K_3-treated hepatocytes and other human cell lines demonstrated that intracellular sulfhydryl groups can be oxidized by Vit K_3 which can lead to the disruption of the cell cytoskeleton, nuclear architecture, plasma membrane and exoplasmic region of the cytoplasm. TRS appear to be fragmented as a result of this treatment. Vit K_3-treatment apparently causes a decrease in the cysteine moieties required during the assembly and regulation of cytoskeleton and hence contribute to the oxidative stress affecting the cells. It is believed that one or more of these effects is responsible for the antitumor activity of Vit K_3. Vit C/Vit K_3 combinations are known to exhibit antitumor activity. Previous work by Taper and his associates demonstrates that when Vit C and Vit K_3 are combined in a ratio of 100:1, the combination exhibits potentiated *in vitro* antitumor activity against MCF-7 (breast carcinoma), KB (oral epidermoid carcinoma), and AN_3-CA (endometrial adenocarcinoma) cell lines as well as *in vivo* antitumor activity in hepatoma-bearing mice (De Loecker *et al.*, 1993; Noto *et al.*, 1989). Tumor specific antitumor activity was achieved with exposure times as short as 1 hour at doses which were 10-50 times lower than when either vitamin was administered alone. Additional studies using hepatoma-bearing mice as a model have shown that the Vit C/Vit K_3 combination is an effective chemosensitizer and radiosensitizer (Taper *et al.*, 1987; Taper and Roberfroid, 1992). Autopsies of hepatoma-bearing mice have revealed that the Vit C/Vit K_3 combination induces little or no major organ pathology when it is administered alone and no additional systemic and major organ pathology when it is administered in conjunction with radiosensitizers or chemosensitizers (Taper and Roberfroid, 1992). The potentiation and specificity of

the antitumor activity were ascribed to the possible generation of peroxides followed by membrane lipid alteration, DNase activation and DNA destruction by the Vit C and K_3 combination in the catalase-deficient cancer cells (Noto *et al.*, 1989; Taper *et al.*, 1987).

In the current study, an MTT assay was employed to demonstrate that the Vit C-Vit K_3 combinations with Vit C:Vit K_3 ratios of 100:1 exhibit synergistic antitumor activity against a human prostatic carcinoma cell line, DU145. A 5 day vitamin treatment of the DU145 cells resulted in CD_{50} values of 2,455 μM for Vit C, 12.9 μM for Vit K_3 and 122 μM ; 1.22 μM for the Vit C/ Vit K_3 combination. These results represent a 20-fold decrease of the CD_{50} of Vit C and a 10-fold decrease in the CD_{50} of the Vit K_3. The MTT assay has also been employed to evaluate the antitumor activity of Vit C, Vit K_3 and the Vit C/Vit K_3 following a 1 hour treatment. Following a 1 hour exposure of the DU145 cells to the vitamins, the CD_{50} values of Vit C, Vit K_3 and the Vit C/Vit K_3 combination are 6009 μM, 77.2 μM and 312 μM/3.12 μM respectively. These values correspond to a 20-fold decrease in the CD_{50} value of Vit C, a 25-fold decrease in the CD_{50} value of Vit K_3. Recently, similar results have been obtained for two bladder carcinoma cell lines, RT4 and T24. Exposure of two of the three cell lines (DU145 and T24) to varying doses of exogenous catalase prior to vitamin treatment abrogated the antitumor activity of the vitamins. The amount of catalase required to destroy the antitumor activity of Vit K_3 alone was greater than or equal to the amount of catalase required to destroy the antitumor activity of the Vit C/Vit K_3 combination. The results of these studies demonstrated that while hydrogen peroxide is involved in the mechanism of action of these vitamins, the enhanced antitumor activity of the Vit C/ Vit K_3 combination was not simply due to the increased production of hydrogen peroxide (Venugopal *et al.*, 1995a,b, submitted).

The close agreement between the CD_{50} values of the Vit C/Vit K_3 combination for the 1 hour vitamin exposure (312 μM/ 3.12 μM) and the CD_{50} values of the Vit C/Vit K_3 combination for the 5 day exposure (122 μM/ 1.22 μM) suggested that a 1 hour treatment was almost as effective as a continuous 5 day vitamin treatment. These results suggest that some of the events responsible for triggering tumor cell death occurred during the first hour of vitamin treatment and may be caused by oxidative stress and cell injury (Martin, 1993). As an initial step in elucidating these processes, SEM and TEM have been employed to examine vitamin-induced changes in DU145 ultrastructure following a 1 hour exposure to the vitamins.

Treatment of DU145 cells by Vit C/Vit K_3 combination exacerbates the individual effects of either vitamins by altering nucleoli and key cytoplasmic organelles [i.e., mitochondria; Fig. 24; lysosome, Figs. 23 and 27; Allen (1987)], stress filaments (i.e., superficial cytoskeleton Figs. 21, 26 and 29), and other cytoskeletal structures (i.e., intermediate filaments and/or microtubules; Fig. 22). In addition, degranulation of RER is characteristic of an early cell damage (Reid *et al.*, 1970).

A second type of cell death begins to appear after 24 hours and reaches its peak 4-5 days following vitamin treatment. As an initial step in elucidating these processes, SEM and TEM have also been employed to examine vitamin-induced changes in DU145 ultrastructure following a 1 hour exposure to the vitamins and a subsequent 24 hour incubation in culture medium (in preparation). Additional experiments designed to evaluate cellular catalase and superoxide dismutase levels as well as the effects of these vitamins on cellular levels of thiols are in progress.

Acknowledgements

This research has been fully supported by a grant from Summa Health System Foundation, Akron, OH, U.S.A. This paper was a part of an invited presentation given at the Scanning Microscopy/1994 meeting in Toronto, Canada, in honor of the retirement of Professor Etienne de Harven from the Banting Institute.

References

Allen TD (1983) The application of scanning electron microscopy to cells in culture: selected methodologies. Scanning Electron Microsc. **1983**; IV, 1963-1972.

Allen TD (1987) Ultrastructural aspects of cell death. In: Perspectives on Mammalian Cell Death. Potten CS (ed.). Oxford Univ. Press, Oxford, UK. pp. 39-65.

Alley MC, Scudiero DA, Monks A, Hursey ML, Czerwinskis MJ, Abbott BJ, Mayo JG, Shoemaker RH, Boyd MR (1988) Feasibility of drug screening with panels of human tumor cell lines using microtiter tetrazolium assay. Cancer Res. **48**, 589-601.

Bellomo G, Mirabelli F, Vairetti M, Iosi F, Mallorni W (1990) Cytoskeleton as a target in menadione-induced oxidative stress in cultured mammalian cells. Biochemical and immunocytochemical features. J. Cell Physiol. **143**, 118-128.

Bram S, Froussard P, Guichard M, Jasmin C, Augery Y, Sinoussi-Barre F, Wray W (1980) Vitamin C preferential toxicity for malignant melanoma cells. Nature **284**, 629-631.

Carruba G, Pavone C, Pavone-Macalusa M, Mesiti M, d'Aquino A, Vita G, Sica G, Castagnetta L (1989)

Morphometry of in vitro systems. An image analysis of two human prostate cancer cell lines (PC-3 and DU145). Pathol. Res. Pract. **185**, 704-708.

Chakraborty J, Von Stein GA (1986) Pleomorphism of human prostatic cancer cells (DU145) in culture - the role of cytoskeleton. Exp. Mol. Path. **44**, 235-249.

Chlebowski RT, Akman SA, Block JB (1985) Vitamin K in the treatment of cancer. Cancer Treat. Rev. **12**, 49-63.

De Loecker W, Janssens J, Bonte J, Taper HS (1993) Effects of sodium ascorbate (Vitamin C) and 2-methyl-1,4-naphthoquinone (Vitamin K_3) treatment on human tumor cell growth *in vitro* II. Synergism with combined action. Anticancer Res. **13**, 103-106.

Gant TW, Rao DN, Mason RP, Cohen GM (1988) Redox cycling and sulphydryl arylation; their relative importance in the mechanism of quinone cytotoxicity to isolated hepatocytes. Chem. Biol. Interact. **65**, 157-173.

Gaylarde P, Sarkany I (1968) Ruthenium tetroxide for fixing and staining cytoplasmic membranes. Science **161**, 1157-1158.

Gilloteaux J, Naud J (1979) The zinc iodide-osmium tetroxide staining-fixative of Maillet. Nature of the precipitate studied by X-ray microanalysis and detection of Ca^{2+} affinity subcellular sites in a tonic smooth muscle. Histochemistry **63**, 227-243.

Ghadially F (1988) Ultrastructural Pathology of the Cell and Matrix. Vol. 1. 3rd edition. Butterworths, London, U.K. pp. 462-477 and 573-587.

Glauert AM (1984) Fixation, Dehydration, and Embedding of Biological Specimens. Vol. 3. North-Holland Publ. Co., Amsterdam. pp. 24-25.

Hayat MA (1970) Principles and Techniques of Electron Microscopy. Biological Applications. Vol. 1. Van Nostrand Reinhold Co, New York. pp. 35-59.

Kessel RG (1968) Annulate lamellae. J. Ultrastruct. Res. Suppl. **10**, 1-82.

Kessel RG (1973) Structure and function of the nuclear envelope and related cytomembranes. In: Progress in Surface Membrane Science. Vol. 6. Danielli JF, Rosenberg MD, Cadenhead DA (eds.). Academic Press, New York. pp. 243-329.

Kessel RG (1983) The structure and function of annulate lamellae: porous cytoplasmic and intranuclear membranes. Int. Rev. Cytol. **82**, 181-303.

Liotti FS, Menghini AR, Guerrieri P, Talsea V, Bodo M (1984) Effects of ascorbic acid and dehydroascorbic acid on the multiplication of tumor ascites cells *in vitro*. J. Cancer Res. Clin. Oncol. **108**, 230-232.

Lupulescu A (1992) Ultrastructure and cell surface studies of cancer cells following vitamin C treatment. Exp. Toxic Pathol. **44**, 3-9.

Malorni W, Iosi F, Mirabelli F, Bellomo G (1991) Cytoskeleton as a target in menadione-induced oxidative stress in cultured mammalian cells: Alterations underlying surface bleb formation. Chem. Biol. Interactions. **80**, 217-236.

Martin SJ (1993) Apoptosis: suicide, execution or murder. Trends Cell Biol. **3**, 141-144.

Mirabelli F, Salis A, Vairetti M, Belloma G, Thor H, Orrenius S (1989) Cytoskeletal alterations in human platelets exposed to oxidative stress are mediated by oxidative and Ca^{2++} dependent mechanisms. Arch. Biochem. Biophys. **270,** 478-488.

Moon TD (1992). Prostate cancer. J. Am. Geriatr. Soc. **40**, 622-627.

Noto V, Taper HS, Yi-Hua J, Janssens J, Bonte J, Loecker WD (1989) Effects of sodium ascorbate (Vit C) and 2-methyl-1,4-napthoquinone (Vit K_3) treatment on human tumor cell growth *in vitro*. Cancer **63**, 901-906.

Nutter LM, Cheng AL, Hung HL, Hsieh RK, Ngo EO, Liu TW (1991) Menadione: spectrum of anticancer activity and effects on nucleotide metabolism in human neoplastic cell lines. Biochem. Pharmacol. **41**, 1283-1292.

Orenstein JM (1992) Ultrastructural pathology of human immunodeficiency virus infection. Ultrastruct. Pathol. **16**, 179-210.

Park CH, Amare M, Savin MA, Hoogstraten B (1980) Growth suppression of human leukemic cells *in vitro* by L-ascorbic acid. Cancer Res. **40**, 1062-1065.

Pavelic K, Kos Z, Spaventi S (1989) Antimetabolic activity of L-ascorbic acid in human and animal tumors. Int. J. Biochem. **21**, 931-935.

Prasad KN, Sinha PK, Ramanujam M, Sakamoto A (1979) Sodium ascorbate potentiates the growth inhibitory effect of certain agents on neuroblastoma cells in culture. Proc. Natl. Acad. Sci. **76**, 829-832.

Prince JS, Kohen C, Kohen E, Jimenez J, Brada Z (1993) Direct connection between myelinosomes, endoplasmic reticulum and nuclear envelope in mouse hepatocytes grown with the amphiphilic drug, quinacrine. Tissue & Cell **25**, 103-110.

Reid IM, Shinozuka H, Sidransky H (1970) Polyribosomal disagreggation induced by puromycin and its reversal with time. An ultrastructural study of mouse liver. Lab. Invest. **23**, 119-127.

Schwarzacher HG, Wachtler F (1993) The nucleolus. Anat Embryol. **188**, 515-536.

Stein O, Stein Y (1971) Light and electron microscopy radioautography of lipids: techniques and biological applications. Adv. Lipid Res. **9**, 1-72.

Stubberfield CR, Cohen GM (1989) A cellular response to quinone-induced oxidative stress in isolated hepatocytes. Biochem. Pharmacol. **38**, 2631-2637.

Sühnel J (1990) Evaluation of synergism and antagonism for combined action of antiviral agents. Antiviral Res. **13**, 23-39.

Taper HS, Roberfroid M (1992) Non-toxic sensitization of cancer chemotherapy by combined vitamin C and K_3 pretreatment in a mouse tumor resistant to oncovin. Anticancer Res. **12**, 1651-1654.

Taper HS, de Gerlache J, Lans M, Roberfroid M (1987) Non-toxic potentiation of cancer chemotherapy by combined C and K_3 vitamin pre-treatment. Int. J. Cancer **40**, 575-579.

Wu FY-H, Liao W-C, Chang H-M (1993) Comparison of antitumor activity of vitamins K_1, K_2 and K_3 on human tumor cells by two (MTT and SRB) cell viability assays. Life Sci. **52**, 1797-1804.

Discussion with Reviewers

W.H. Wilborn: You have described an interesting and important effect of a vitamin C-vitamin K_3 combination on DU145 cells, a human prostatic cancer cell line. Why have you not quantified your findings for the vitamins alone and for the combination of vitamins? The means are readily available and the data would add significance to your study?

Authors: The quantitative analysis of each vitamin and their combination in terms of cytotoxicity was presented at the National Meeting of the Basic Urologic Research held in San Francisco (May 1994) and has been submitted to another scientific journal.

A. Reith: On what ground did you limit your SEM and TEM observations to a "one hour" incubation with combined vitamins?

Authors: The "one hour" incubation was chosen as model for a potential and practical urologic treatment. Our experimental results have shown that a "one hour" treatment is as effective as a longer duration treatment (up to 5 days). This longer treatment does not improve significantly the cytotoxic effect found after "one hour" treatment (see Table 1 and **Discussion**).

A. Reith: To conclude that your observations suggest an effect of the vitamins on the cytoskeleton of the DU145 cells takes a solid stretch of the imagination since no cytoskeletal element is demonstrated in any of your micrographs! Even the evidence presented for cytoplasmic blebs is rather weak. Still, it is on these blebs that you based a suggestion for a cytoskeletal effect (legend of Figs. 14 and 15). Please clarify.

Authors: We agree with the comments of the reviewer that we have only indirect evidences for the cytoskeletal damages induced by the vitamins. These include characteristic morphological changes viewed with the SEM: (a) cell surface and superficial, cytoplasmic morphology are directed and/or influenced by the architectural arrangement of stress (actin and associated proteins) filament complexes (blebs); (b) the cytoskeletal intermediate filament damages can affect the overall shape of the cell, the integrity and the positioning of the nucleus and its adjacent area. Additional information has been provided with the TEM. These observations support the filopodial changes due to the absence or defect of axial supportive structures. In most cases, the filopodia appear short. When elongated, they are irregularly-shaped and entangled as if a network was created by the lack of organized stress filaments and cytoskeleton. Mitochondrial damage can lead to the depletion of cell energy charge [Atkinson DE (1968) The energy charge of the adenylate pool as a regulatory parameter. Interactions with feedback modifiers. Biochemistry **7**, 4030-4040] and this in turn contributes to the membrane leaks and defects. In addition, it can prevent polymerization and maintenance of actin and of other important cytoskeletal structures. We agree that we have not reported any image about the microtubules in this report but our morphological studies are in progress and we plan to report about this in future.